



Prediction of thermal conductivity of liquid and vapor refrigerants for pure and their binary, ternary mixtures using artificial neural network

N. Ghalem, S. Hanini, Mx Naceur, M Laidi, Abdeltif Amrane

► To cite this version:

N. Ghalem, S. Hanini, Mx Naceur, M Laidi, Abdeltif Amrane. Prediction of thermal conductivity of liquid and vapor refrigerants for pure and their binary, ternary mixtures using artificial neural network. *Thermophysics and Aeromechanics*, 2019, 26 (4), pp.561-579. 10.1134/S0869864319040085 . hal-02515141

HAL Id: hal-02515141

<https://univ-rennes.hal.science/hal-02515141>

Submitted on 23 Mar 2020

HAL is a multi-disciplinary open access archive for the deposit and dissemination of scientific research documents, whether they are published or not. The documents may come from teaching and research institutions in France or abroad, or from public or private research centers.

L'archive ouverte pluridisciplinaire **HAL**, est destinée au dépôt et à la diffusion de documents scientifiques de niveau recherche, publiés ou non, émanant des établissements d'enseignement et de recherche français ou étrangers, des laboratoires publics ou privés.

1 **Prediction of Thermal Conductivity of Liquid and Vapor Refrigerants for**
2 **Pure and their Binary, Ternary Mixtures using Artificial Neural Network**

3

4 N. Ghalem¹, S. Hanini², M. W. Naceur¹, M.Laidi², A. Amrane^{3*}

5

6 ¹Département de Chimie Industrielle Université de Blida

7 ²LBMP, Université de Médéa, Quartier Ain D'Heb, 26000, Médéa, Algérie.

8 ³Ecole Nationale Supérieure de Chimie de Rennes, Université de Rennes 1, CNRS, UMR

9 6226, 11 allée de Beaulieu, CS 50837, 35708 Rennes Cedex 7, France.

10

11 *Phone : +33 223 23 81 55 ; Fax : +33 223 23 80 99 ; email : abdeltif.amrane@univ-
12 rennes1.fr

13

14 **Abstract**

15 The determination of thermophysical properties of hydrofluorocarbons (HFCs) is very
16 important, especially the thermal conductivity. The present work, investigated the potential of
17 an artificial neural network (ANN) model to correlate the thermal conductivity of (HFCs) at
18 (169.87-533.02) K, (0.047-68.201) MPa and (0.0089- 0.1984) W.m.⁻¹K⁻¹ temperature,
19 pressure and thermal conductivity ranges respectively, of 11 systems from 3 different
20 categories including five pure systems(R32, R125, R134a,R152a,R143a),four binary mixtures
21 systems(R32+R125, R32+R134a, R125+ R134a,R125+R143a), and two ternary mixtures
22 systems (R32+R125+ R134a, R125+ R134a+ R143a).Each one received 1817,794 and 616
23 data points, respectively.The application of this model for these 3227 data points of liquid and
24 vapor at several temperatures and pressures allowed to train, validate and test the model. This

25 study showed that ANN models represent a good alternative to estimate the thermal
26 conductivity of different refrigerant systems with a good accuracy. The squared correlation
27 coefficients of thermal conductivity predicted by ANN were $R^2 = 0.998$ with an acceptable
28 level of accuracy of RMSE = 0.0035 and AAD = 0.002 %. The results of applying the trained
29 neural network model to the test data indicate that the method has a highly significant
30 prediction capability.

31

32 **Key words:** Refrigerant, Pure system, Mixtures, Thermal conductivity, Artificial Neural
33 Network, Predictive model.

34

35 **Introduction**

36 In recent years, It has been highlighted the need to establish a balance between "energy
37 consumption" and "environmental protection". The introduction of new refrigerants to replace
38 Chlorofluorocarbons (CFCs) and Hydrochlorofluorocarbons(HCFCs) and the adaptation of
39 new techniques should allow a reduction of the overall environmental impacts. To reduce
40 security risks, another line of research has been developed towards the use of a secondary
41 cooling loop (indirect cooling). The multiple processes used in industry are often based on
42 heat exchanges.

43 Refrigerants cause global warming and ozone depletion bring on the environmental problems.
44 So, UN drew up the Montreal Protocol(MP) and its London and Copenhagen
45 Amendments[1]. Prior to the 1980s, the principal classes of chemicals used as refrigerants in
46 the refrigeration industry were CFCs and HCFCs. Based on growing evidence of ozone
47 depleting potential (ODP)[2] of CFCs based on the Montreal Protocol, different industries
48 turned to HCFCs as substitutes for CFCs. While HCFCs have a lower ODP than CFCs, they
49 still damage the ozone layer and have become topic to scheduled period out by 2030,

50 Hydrofluorocarbons (HFCs) were used as an acceptable alternative to CFCs and HCFCs
51 because they possess several characteristics, including near-zero ODP and low Global
52 warming potential (GWP), similarity to CFCs and HCFCs in physical properties, short
53 atmospheric lifetimes, less or non-flammable and not expensive [3].

54 During the previous periods, owing to the understanding of the impact of refrigerants in the
55 destruction of the ozone layer, the concepts of ozone depletion potentials (ODPs)[4]was
56 designedto determine the relative capacity of a chemical to destroy ozone, [5,6,7,8].
57 Consequently, GWP is the purpose of several studies leading to the publication of a wide
58 range of literature data [9].

59 Many researchers focused their efforts on the measurement of the thermophysical properties
60 of these compounds (Refrigerants), aiming to find proper substitutes. Thermal conductivity is
61 one of the major thermophysical properties, as defined by Fourier's equation, it is the ability
62 of a material to transmit heat by means of conduction. Thermal conductivity, K ($\text{W. m}^{-1}\text{K}^{-1}$),
63 is essential to theknowledge of heat transfer, in particular for refrigerants. In fact, the higher
64 the liquid and vapor thermal conductivity, the higher the heat transfer coefficient.

65 The context of this work is related to the problem of the substitution of CFC and HCFCs.
66 Experimental aspect (technical and measurements) and modeling aspects of the data obtained
67 were first considered. The products studied are mixtures (pure, binary and ternary)
68 compounds of R32, R125, R134a, R152a and R143a, which are HFCs of high interest to the
69 industries of air conditioning and refrigeration.

70 Different authors have used diverse equations and methods to predict and reproduce the
71 thermodynamic properties of refrigerant systems. Most of these attempts have been restricted
72 to limited systems and to the best of the knowledge of no systematic work devoted to test the
73 ability of these methods to predict the thermodynamic properties of different categories of
74 systems is available. A number of theories are available providing equations to predict the

75 thermal conductivity of liquids, these equations include theoretical calculations which
76 consider intermolecular distances [10]; there are equations based on the theory of group
77 contribution [11] or molecular descriptors [12,13]; equations involving some fixed parameters
78 in order to describe the thermal conductivity [12,14]. An empirical approach based on a
79 limited number of fixed physical parameters [15] was considered; a new equation to describe
80 the thermal conductivity of R-32, R-125, R134a, and R-143a for practical use, applicable over
81 a wide range of temperature and pressure has also been proposed [16]. Semi-empirical
82 approaches for correlating thermal conductivity data for multicomponent liquid mixtures
83 [17,18] were studied, a method to estimate the thermal conductivity and the viscosity similar
84 to cubic equations of state of halogenated hydrocarbon of pure substances in vapor and liquid
85 regions [19,20] was proposed; thermal conductivity modeling of refrigerant mixtures in a
86 three-parameter corresponding states format [21] was carried out. There are an extensive
87 studies have been published in the literature on the thermal conductivity of mixed refrigerants
88 [22,23,24] which suggested a correlation to calculate the thermal conductivity and viscosity of
89 some alternative refrigerant mixtures such as R-507, R-404A, R-407C, and R-410A.

90 Recently, some researchers used artificial neural networks (ANNs) to correlate thermal
91 conductivity property [25]:and obtained much better results than the traditional approach. To
92 minimize the difficulties of experimental measurements and also their time-consuming and
93 costly nature, it is desirable to develop predictive methods for estimating the phase behavior
94 of these kinds of systems.

95 The purpose of this study was therefore the application of artificial neural network for
96 representing/predicting the liquid and vapor thermal conductivity of pure refrigerants
97 including R32, R125, R134a, R152a, R143a and their binary, ternary mixtures at different
98 temperatures and pressures.

99 **Methodology and modeling**

100 **Neural network**

101 Artificial neural networks (ANNs) consist of a number of neurons working in unity to solve
102 various scientific and engineering problems such as estimation of physical and chemical
103 properties [26].ANN can operate like a black box model, which requires no detailed
104 information about the system or equipment. The ANN can learn the relationship between
105 input and output based on the training data.

106 ANNs have been used in many engineering applications such as control systems, in
107 classification and in modeling complex process transformations. Detailed information about
108 artificial neural networks can be found in the following References [27,28]. ANNs is a widely
109 used numerical method which is able to model any kind of data set even complex ones.

110 **Selection of network parameters**

111 The artificial neurons are arranged in layers where in the input layer receive inputs (u_i),
112 namely experimental data and each succeeding layer receives weighted outputs (w_{ij} , u_i) from
113 the preceding layer as its input resulting therefore a feedforward ANN, in which each input is
114 feed forward to its succeeding layer where it is treated. The outputs of the last layer constitute
115 the outputs to the real world [29]. In such a feed forward ANN a neuron in a hidden or an
116 output layer has two tasks:

117 (a) It sums the weighted inputs from several connections plus a bias value and then applies a
118 transfer function to the sum as given by (for neuron j of the hidden layer):

$$119 z_j = f_h(\sum_{i=1}^n w_{ji}^I u_i + b_{hj}); j = 1, 2, \dots, m \quad (1)$$

120 (b) It propagates the resulting value through outgoing connections to the neurons of the
121 succeeding layer where it undergoes the same process as given by (for instance outputs Z_j of
122 the hidden layer fed to neuron k of the output layer gives the output V_k):

$$123 V_k = f_o(\sum_{j=1}^m w_{kj}^h z_j + b_{0k}); k = 1, 2, \dots, i \quad (2)$$

124 Combining equations 1 and 2 the relation between the output V_k and the inputs u_i of the NN is
125 obtained:

126
$$V_k = f_0 \left(\sum_{j=1}^m w_{kj}^h f_h \left(\sum_{i=1}^n w_{ji}^l u_i + b_{hj} \right) + b_{ok} \right); k=1, 2 \dots , i \quad (3)$$

127 The output is computed by means of a transfer function, also called activation function. It is
128 desirable that the activation function has a sort of step behavior. Furthermore, because
129 continuity and derivability at all points are required features of the current optimization
130 algorithms[30,31,29] three kinds of transfer function are considered in this study:

131 Hyperbolic tangent sigmoid transfer function:

$$f(a) = \frac{e^a - e^{-a}}{e^a + e^{-a}} \quad (4)$$

132 Logarithmic sigmoid transfer function:

133
$$f(a) = \frac{1}{1+e^{-a}} \quad (5)$$

134 Pure linear transfer function:

135
$$f(a) = a \quad (6)$$

136 **Training of network**

137 A Feed forwardback propagation (FFBP) which is very effective in representing nonlinear
138 relationships among variables was used in this work BP algorithm (BPA) is the most widely
139 used in ANN, and has different variants. FFBP with Levenberg-Marquardt (BP) training
140 algorithm and one hidden layer was chosen because it is suitable for modeling the relationship
141 between input data and output variable[32].

142 **Testing of network**

143 The criteria used for measuring the performance of the network are the absolute fraction of
144 variation (R^2), and the root mean square error (RMSE), which can be calculated using the
145 following equations.

146 The fraction of absolute variance is given by:

147

$$R^2 = 1 - \frac{\sum_{i=1}^N (K_{cal,i} - K_{exp,i})^2}{\sum_{i=1}^N (K_{exp,i})^2} \quad (7)$$

148 The root mean square error value is calculated by

149

$$RMSE = \sqrt{\sum_{i=1}^N (K_{cal,i} - K_{exp,i})^2 / N} \quad (8)$$

150 Here, N is the number of data patterns in the independent data set, $K_{cal,i}$ indicates the values
151 predicted by ANN, $K_{exp,i}$ is the measured value of one data point i[33,34].

152 The accuracy of the model to reproduce and predict the thermal conductivity of refrigerant
153 systems at different temperatures and pressures may be evaluated using the statistical
154 parameters [35,36]: namely, the absolute average deviation(AAD), and the mean square error
155 (MSE) which are defined as follows:

156 The mean square error value is calculated according to:

157

$$MSE = \frac{1}{N} \sum_{i=1}^N (K_{exp,i} - K_{cal,i})^2 \quad (9)$$

158 The absolute average deviation value is calculated by[29]:

159

$$AAD = \frac{1}{N} \sum_{i=1}^N |K_{exp,i} - K_{cal,i}| \quad (10)$$

160 The Average Absolute Relative Deviation:

161

$$AARD\% = \frac{100}{N} \sum_{i=1}^N \left| \frac{K_{exp,i} - K_{cal,i}}{K_{exp,i}} \right| \quad (11)$$

162 **Optimization of the network architecture**

163 Optimization of the network architecture is the major task in ANN. The parameters that affect
164 the performance of the network are the number of neurons in the hidden layer, the number of
165 hidden layers, the transfer function and the training algorithm. The network architecture can
166 be optimized by varying the above parameters (using trial and error method) to achieve the
167 results with good accuracy [33,34].

168

169

170 **Results and Discussion**

171 In the present study, a total of 3227 data points of thermal conductivity data were considered.
172 The collected experimental data points were divided into three different sub- datasets five
173 pure systems, (R32, R125, R134a, R152a, R143a), four binary mixtures systems(R32+R125,
174 R32+R134a, R125+ R134a, R125+R143a), and two ternary mixtures systems (R32+R125+
175 R134a, R125+ R134a+ R143a) at several temperatures and pressures. Each one received 1817,
176 794, 616 data points respectively.

177 For developing the neural network model, inputs and outputs should be first defined. The
178 input parameters included, Temperature (T (k)) and pressure (P (MPa)),namely two
179 macroscopic inputs which characterize the physical conditions of the system. Molecular
180 weight (M (g. mol⁻¹)), critical temperature (T_c (k)), critical pressure (P_c (MPa)), critical density
181 (D_c (Kg. m⁻³)), and mass fraction of liquids or vapor phase (X) were the other selected inputs
182 for pure systems they were specified as pseudo critical mixtures property for binary and
183 ternary systems(9 inputs), and Thermal conductivity was the network output (1 output).The
184 network is simple in structure and easily analyzed mathematically is schematically illustrated
185 in Fig. 1 and Table1shows the physical properties values of these compounds accompanied
186 with related references. This study employs experimental data from the open literature for
187 each (pure, binary, ternary) systems, the details listed in Tables 2 to 4 respectively.

188 The available correlations for prediction can be described as follows:

$$189 \quad K = f(T, P, M, T_C, P_C, D_C, X_i, X_j, X_k) \quad (12)$$

190 Calculation of the pseudo critical mixtures properties

191 The different equations of state were developed from the knowledge of the properties P , V , T
192 of pure substances. In the case of mixtures of known composition, it is necessary to make use
193 of mixing rules for calculating the average properties of the mixture. Pseudo properties in the
194 case of critical mixtures, are generally obtained from the rule of Kays (1936):

$$195 \quad T_{PC} = \sum_{i=0}^n X_i * T_{Ci} \quad (13)$$

$$P_{PC} = \sum_{i=0}^n X_i * P_{Ci} \quad (14)$$

$$196 \quad D_{PC} = \sum_{i=0}^n X_i * D_{ci} \quad (15)$$

$$M_{PC} = \sum_{i=0}^n X_i * M_{Ci} \quad (16)$$

$$198 \quad K = f(T, P, M_{PC}, T_{PC}, P_{PC}, D_{PC}, X_i, X_j, X_k) \quad (17)$$

199 n=1 for pure refrigerant, $X_i = 1, X_j = 0, X_k = 0$, n=1, 2 for binary mixtures, $X_i + X_j = 1, X_k = 0$
 200 and n=1, 2, 3 for ternary mixtures, $X_i + X_j + X_k = 1$.

201 Procedure for neural network modeling of the thermal conductivity

202 ANN modeling is described consists in the following four steps: (a) extract the results from
203 experiments or theoretical calculations (b) train the network using experimentally or
204 theoretically predicted values(c) testing of network with data, which are not used for
205 training,(d) identify the best network architecture based on statistical performance values
206 [33,34].

207 (i) phase of collection of experimental data as complete as possible. From this, the following
208 procedure was considered:

209 (ii) division of data base to three parts (DB of pure systems, BD of binary systems, BD of
210 ternary systems)

211 (iii) phase of pre-treatment and analysis of the data.

212 (iv) dividing data into three subsets-train, validation and test.

(v) phase of choice of the parameters of the neural network (neural network (FFBP), neurons number in hidden layer, activation function in hidden layer (tan-sig), activation function in output layer(Tang-sig)).

216 (vi)saving the parameters of the optimal ANN.

217 Table 5 shows the structure of the optimized ANN model for each pure systems, binary
218 systems, ternary systems and global systems *Tan-sig* is a sigmoid transfer function used in the
219 hidden layer and used in the output layer for all systems, in this table, R² values and RMSE of
220 the trained networks have been shown for different number of hidden layer neurons. The best
221 configuration with minimum error measure (RMSE) and appropriate R² value. The
222 parameters (weight and biases values) of the best selected NN model for each system (pure,
223 binary, ternary, global) are listed in Tables 6 to 9 respectively, where W^I is the input-hidden
224 layer connection, W^h is the hidden layer output connection, b_{hj} and b_{0k} are biases of the neuron
225 j of the hidden layer and the neuron of the output layer respectively.

226 Table 10 shows the regression line of the network model equation during training, validation,
227 and prediction sets of pure systems, binary systems, ternary systems and global system
228 RMSE, MSE, AAD, AARD, and SSE, are collected in Table 11 showing that there was a
229 significant correlation between experimental and predicted values. For each plot, the ANN
230 method provide good results with high correlation coefficients (R²_{exp}, R²_{cal}). Comparison
231 between the output data and calculated values of the thermal conductivity of different
232 refrigerant systems with (R²_{pure} = 0.997, R²_{binary} = 0.998, R²_{ternary} = 0.998, R²_{global} = 0.997), shows
233 slopes close to unit and an intercept values close to zero, confirming the agreement between
234 experimental and predicted values (Fig. 2).

235 **Reduction technique**

236 The reduced data refers to the analysis and transformation of the input and target variables
237 having different physical units with different range values in order to minimize the input
238 parameters (9 inputs to 7 inputs) and to improve the learning quickness, the present study use
239 this method to calculate the minimum and the maximum of each vector variable and scaling
240 the data with respect the upper limits. Finally, the values of the outputs from the neural
241 network reduced are converting before being presented.

242 For data reduce, the following equations are considered:

$$G_r = \frac{G - G_{min}}{G_{max} - G_{min}} \quad (17)$$

243 $X_i = X_i + 1$ (18)

244 $T_r = \frac{T}{T_c}, P_r = \frac{P}{P_c}$ (19)

245 For converting (to real value) of data estimated by ANN:

246 $G = G_r * (G_{max} - G_{min}) + G_{min}$ (20)

$$K = f(T_r, P_r, M_r, D_r, X_i, X_j, X_k) \quad (21)$$

247 Where G is the original data value, G_r is the corresponding reduced variable; min, max are the
248 minimal and the maximal values of each vector respectively.

249 The validation agreement, coefficients of determination(R^2_{exp}) and (R^2_{cal}), and different
250 errors values RMSE, MSE, AAD, AARD, and SSE, are collected in Table 12. The
251 performance of the present developed ANN (RN2, RN3) models were compared to the
252 previously developed ANN models (RN1) to estimate the thermal conductivity for original
253 (real) data and also the reduced data. The three models provided high values of the correlation
254 coefficient R^2 , as illustrated in Fig. 3 otherwise the RN1 model obtained was similar to RN3;
255 while the RN2 model led to a better fit of experimental data than the RN1, RN3 models.

256 Artificial neural network prediction

257 The assembled of new experimental data points, namely 660 data points, for harmful
258 refrigerants covered thermal conductivity range 0.0106-0.15 W/m. K, temperature range of
259 164.77–463K, and pressure range of 0.059–69.58 MPa. These collected data were distributed
260 into 363 data points for three pure systems (R22, R124, R142b), 240 data points for two
261 binary systems (R22+R142b, R22+R152a) and 57 data points for one ternary system
262 (R142b+R124+R22). In this part the range of experimental data parameters and the number of

263 data points accompanied with their references in Tables13, 14 and 15 for different systems
264 (pure ,binary, ternary),respectively.

265 The prediction of the new data base(DB2) of the harmful refrigerants by no harmful
266 refrigerants using (DB1) are given in Fig.4 this indicates that the new approach (RN3)
267 improved the prediction of thermal conductivity, producing the following RMSE, MSE,
268 AAD, AARD, SSE and R² values, 0.0123, 0.0002, 0.0094%, 17.92%, 0.10 and 0.974,
269 respectively (Table 16).

270 These results show the good predictive ability of the ANN model. In general, in Fig. 5 the
271 residual did not exceed -0.025 to 0.04 for new data base (DB2) and ± 0.02 for data base
272 (DB1),(except for a few experimental points).The illustration of harmful refrigerants for all
273 (pure, binary, ternary) systems by different colors that shows an appropriateR² value,
274 0.95,are shown in Fig. 6 this confirms that the method out performs prediction ability.
275 Fig.7shows the prediction of DB2 by DB1 in the range [0.01, 0.03]W.m⁻¹. K⁻¹.

276 All experimental data points (DB1+DB2), namely the whole 3887 data points, were divided
277 into three different sub- datasets: eight pure systems, (R32, R125, R134a, R152a, R143a, R22,
278 R124, R142b), six binary mixtures (R32+R125, R32+R134a, R125+ R134a, R125+R143a,
279 R22+R142b, R22+R152a), and three ternary mixtures (R32+R125+ R134a, R125+ R134a+
280 R143a, R142b+R124+R22), namely 2180, 1034, 673 data points respectively.

281 Figs. 8,9 and Table 17 shows a significant correlation with percentage residual error varying
282 in the range of ± 0.02 , a high R² value, 0.998, and fairly accurate prediction the absolute
283 average deviation error (AARD), estimated to be 5.8%, as well as a high robustness.

284

285 Conclusion

286 In this paper, a methodology for choosing an ANN model to predict thermal conductivity was
287 presented. The methodology starts with a wide search in order to select the model with

288 minimum complexity, optimal performance and choice of the respective parameters (inputs
289 and outputs, activation functions, training algorithm, reduction technique, hidden layers).

290 An artificial neural network model was used to predict the thermal conductivity of pure
291 refrigerants and their binary, ternary mixtures for liquid and vapor phaseof11 systems from 3
292 different categories containing five pure systems (R32, R125, R134a, R152a, R143a), four
293 binary mixtures(R32+R125, R32+R134a, R125+ R134a, R125+R143a) and two ternary
294 mixtures (R32+R125+ R134a, R125+ R134a+ R143a).This study involved 3227 data points
295 including the temperature, the pressure, the molecular weight, the critical temperature, the
296 critical pressure, the critical density and the mass fraction of liquid and vapor phases of
297 refrigerants.

298 In this work, the feed forward Backpropagation (BP) algorithm with Levenberg–
299 Marquardt(LM) training was applied to estimate the thermal conductivity. One relevant model
300 (RN1) we attempted to improve their performance by using the reduction technique to attain
301 (RN3).The best network model obtained consisted of the best fit of the validation agreement
302 plot, and high R^2 value,0.997was obtained. Furthermore, the statistical analysis showed that
303 the model (RN3) was able to yield quite satisfactorily estimates for pure, binary and, ternary
304 refrigerant systems, as well as the global system, the model was shown to be robust.

305 The performance of the proposed ANN model was also examined through its application to
306 test a data set consisting of 660 experimental points of thermal conductivity for various
307 systems for diverse pure, binary and ternary mixtures of refrigerants over a wide range of
308 temperatures and pressure. The results of this evaluation indicate that the developed ANN
309 model was capable to predict thermal conductivity with a high coefficient of determination.
310 The results of applying the trained neural network model to the test data indicate that the
311 method has a very good prediction capability with respect to not only the temperature and
312 pressure ranges but also the refrigerant types.

313 Lastly the gathering of all experimental data points DB1and DB2 (RN4)gave a high R^2 value,
314 0.998, and a low average absolute relative deviation error (5.8%).

315 **Nomenclature**

316 AAD Average absolute deviation
317 AARD Average absolute relative deviation
318 ANN Artificial neural network
319 CFCs Chlorofluorocarbons
320 FFBP Feed forward back propagation
321 GWP Global warming potential
322 HCFCs Hydrochlorofluorocarbons
323 HFCs Hydrofluorocarbons
324 M Molecular mass ($\text{g} \cdot \text{mol}^{-1}$)
325 M_c Critical molecular mass ($\text{g} \cdot \text{mol}^{-1}$)
326 MSE Mean square error
327 N Number of data points
328 ODP Ozone depleting potential
329 P Pressure (MPa)
330 P_c Critical pressure (MPa)
331 R^2 Coefficient of determination
332 regression equation
333 RMSE Root mean square error
334 T Temperature (K)
335 T_c Critical temperature (K)
336 W Weights
337 X Mass fraction of liquid or vapor phase
338 α Slope of the linear regression
339 equation
340 β y Intercept of the linear regression
341 equation
342 *Subscripts/superscripts*

343 Cal Calculated
344 exp experimental
345 max maximum
346 min minimum
347 n component
348 * harmful refrigerant

349 *Greek letters*

350 K Thermal conductivity ($\text{W} \cdot \text{m}^{-1} \cdot \text{K}^{-1}$)
351 D Density ($\text{Kg} \cdot \text{m}^{-3}$)

352 D_c Critical density ($\text{Kg} \cdot \text{m}^{-3}$)

353 *Acronyms*

354 ASHRAE American society of heating, refrigerating and air conditioning engineers

355 MP Montreal Protocol

356

357

358 **References**

359

1. World Meteorological Organization, Montreal protocol on substances that deplete the ozone layer report, WMO Bull.,1988, Vol. 37, P. 94–97.
2. J.W. Ramsdell, G.L. Colice, B.P. Ekholm, N.M. Klinger, Cumulative dose response study comparing HFA-134a albuterol sulfate and conventional CFC albuterol in patients with asthma, Ann. of Allergy Asthma Immunol., 1998, Vol. 81, P. 593-599.
3. W.T. Tsai, An overview of environmental hazards and exposure risk of hydrofluorocarbons (HFCs), Chemosphere., 2005, Vol. 61, P. 1539-1547.
4. World Meteorological Organization (WMO), 2007. Scientific Assessment of Ozone Depletion: 2006, Global Ozone, Research and Monitoring Project – Report 50, Switzerland: Geneva.
5. World Meteorological Organization (WMO), (2003), Scientific Assessment of ozone depletion: 2002, Global Ozone, Research and Monitoring Project – Report 47, Switzerland: Geneva.
6. C. H. Bridgeman, J. A. Pyle, D. E. J. Shallcross, A three-dimensional model calculation of the ozone depletion potential of 1-bromopropane (1-C₃H₇Br), Geophys. Res., 2000, Vol. 105 P. 493-426, 502.
7. S. C. Olsen, B. J. Hannegan, X. Zhu, , M. J. Prather, Evaluating ozone depletion from very short-lived halocarbons, Geophys. Res. Lett., 2000, Vol. 27,P. 1475-1478.
8. D. J. Wuebbles, K.O. Patten, M. T. Johnson, R., J. Kotamarthi, The new methodology for ozone depletion potentials of short-lived compounds: n-propyl bromide as an example, Geophys. Res.,2001, Vol. 106, P. 551-571.
9. P. A. Newman, J.S. Daniel, D.W. Waugh, E. R. Nash, A new formulation of equivalent effective stratospheric chlorine (EESC), Atmos. Chem. Phys., 2007, Vol. 7, P. 4537-4552.
10. P.W. Bridgman, conductivity of liquids under pressure, Proc. Am. Acad. Art Sci.,1923, Vol. 59, P. 141-169.
11. S.R.S. Sastri, K.K. Rao, A new temperature thermal conductivity relationship for predicting saturated liquid thermal conductivity, J. Chem. Eng.,1999, Vol. 74, P. 161-169.
12. B.E. Poling, J.M. Prausnitz, J.P. O'Connell, The properties of gases and liquids, fifthed. McGraw-Hill, New York., 2001.
13. F. Gharagheizi, P. Ilani-Kashkouli, M. Sattari, A..H. Mohammadi, D. Ramjugernath, D. Richon, Development of a quantitative structure liquid thermal conductivity relationship for pure chemical compounds, Fluid Phase Equilib., 2013,Vol. 355,P. 52- 80.

14. F. Gharagheizi, P. Ilani-Kashkouli, M. Sattari, A.H. Mohammadi, D. Ramjugernath, D. Richon, Development of a general model for determination of thermal conductivity of liquid chemical compounds at atmospheric pressure, *J. AIChE*, 2013, Vol. 59, P. 1702-1708.
15. G. Di Nicola, E. Ciarrocchi, M. Pierantozzi, R. Stryjek, Anew equation for the thermal conductivity prediction of pure liquid compounds, *J. Therm. Anal. Calorim.*, 2014, <http://dx.doi.org/10.1007/s10973-013-3422-7>.
16. J. Yata, Y. Ueda, M. Hori, Equations for the thermal conductivity of R-32, R-125, R-134a, and R-143a, *Int. J. Thermophys.*,2005, Vol. 26, P. 1423-1435.
17. L. Shi, X. J. Liu, X. Wang, M. S. Zhu, Prediction method for liquid thermal conductivity of refrigerant mixtures, *Fluid Phase Equilib.*, 2000,Vol. 172, P. 293–306.
18. W.W. Focke, Correlating thermal conductivity data for ternary liquid mixtures, *Int. J.Thermophys.*, 2008, Vol. 29, P. 1342–1360.
19. M.G. He, Z.G. Liu, J.M. Yin, New equation of state for transport properties: Calculation for the thermal conductivity and the viscosity of halogenated hydrocarbon refrigerants, *Fluid Phase Equilib.*, 2002, Vol. 201, P. 309–320.
20. M.J. Assael, N.K. Dalaouti, K. E. Gialou, Measurements of the thermal conductivity of liquid R32, R124, R125, and R141b, *Fluid Phase Equilib.*, 2000,Vol. 174, P. 203–211.
21. G. Scalabrin, L. Piazza, M. Grigiante, M. Baruzzo, Thermal conductivity modeling of refrigerant mixtures in a three-Parameter corresponding states format, *Int. J. Thermophys.*, 2005, Vol. 26, P. 399-412.
22. M.L. Huber, D.G. Friend, J.F. Ely, Prediction of the thermal conductivity of refrigerants and refrigerant mixtures, *Fluid Phase Equilib.*,1992, Vol. 80, P. 249-261.
23. M.O. McLinden, S.A. Klein, , R.A. Perkins, An extended corresponding states model for the thermal conductivity of refrigerants and refrigerant mixtures, *Int. J. Refrigeration.*, 2000,Vol. 23, P. 43-63.
24. S.M. Sami, J.D. Comeau, Study of viscosity and thermal conductivity effects on condensation characteristics of some new alternative refrigerant mixtures, *Int. J. Energy Res.*, 2003, Vol. 27, P. 63–77.
25. Y. Islamoglu, A new approach for the prediction of the heat transfer rate of the wire-on-tube type heat exchanger use of an artificial neural network model, *Appl. Therm. Eng.*,2003, Vol. 23, P. 243–249.
26. J. Taskinen, J. Yliruusi, Prediction of physicochemical properties based on neural network modeling, *Adv. Drug. Deliv. Rev.*,2003, Vol. 55, P. 1163-1183.
27. L.H. Tsoukalas, R.E. Uhrig, Fuzzy and neural approaches in engineering. John Wiley et Sons Inc., 1997.

28. S.A. Kalogirou, Applications of artificial neural networks for energy systems, *Appl. Energy.*, 2000, Vol. 67, P. 17–35.
29. C. Si-Moussa, S. Hanini, R. Derriche, M. Bouhedda, A. Bouzidi, Prediction of high-pressure vapor liquid equilibrium of six binary systems, carbon dioxide with six esters, using an artificial neural network model, *Brazilian J. Chem. Eng.*, 2008, Vol. 25, P. 183-199.
30. MY. Rafiq, G. Bugmann, DJ. Easterbrook, Neural network design for engineering applications, *Comput. Struct.*, 2001, Vol. 79, P. 1541–1552.
31. Math Works . Neural network toolbox user's guide.MATLAB7.0, Release 14, MATLAB manual., 2004.
32. A. Witek-Krowiak, K. Chojnacka, D. Podstawczyk, A. Dawiec, K. Pokomeda, Application of response surface methodology and artificial neural network methods in modeling and optimization of biosorption process, *Bioresour Technol.*, 2014, doi:10.1016/j.biortech.2014.01.021.
33. S.A. Kalogirou, Artificial intelligence for the modeling and control of combustion processes, *Prog. Energy. Combust. Sci* 29 (2003) 515–566.
34. A. Mellit, S.A. Kalogirou, Artificial intelligence techniques for photovoltaic applications, a review. *Prog. Energy. Combust. Sci.*, 2008, Vol. 34, P. 574–632.
35. R. Haghbakhsh, H. Adib, P. Keshavarz, M. Koolivand, S. Keshtkari, Development of an artificial neural network model for the prediction of hydrocarbon density at high-pressure, high-temperature conditions, *Termochim. Acta.*, 2013, Vol. 551, P. 124-130.
36. F. Amato, J. L. Gonzalez-Hernandez, J. Havel, Artificial neural networks combined with experimental design: a “soft” approach for chemical kinetics. *Talanta.*, 2012, Vol. 93, P. 72-78.
37. Y. Tanaka, M. Nakata, T. Makita, Thermal conductivity of gaseous HFC-134a, HFC-143a, HCFC-141b, and HCFC-142b, *Int. J. Thermophys.*, 1991, Vol. 12, P. 949-963.
38. G.K. Lavrenchenko, G.Ya. Ruvinskij, S.V. Iljushenko, V.V. Kanaev, Thermophysical properties of refrigerant R134a, *Int. J. Refrigeration.*, 1992, Vol. 15, P. 386-392.
39. R.A. Perkins, A. Laesecke, C.A. Nieto Castrob, Polarized transient hot wire thermal conductivity measurements, *Fluid Phase Equilib.*, 1992, Vol. 80, P. 275-286.
40. U. Gross, Y.W. Song, E. Hahne, Thermal conductivity of the new refrigerants R134a, R152a, and R123 measured by the Transient Hot-Wire method, *Int. J. Thermophys.*, 1992, Vol. 13, P. 957-983.
41. A. Laeseck, R.A. Perkin, C.A. Nieto Castro, Thermal conductivity of R134a, *Fluid Phase Equilib.*, 1992, Vol. 80, P. 263-274.
42. R., Yamamoto, S. Matsuo, Y. Tanaka, Thermal conductivity of halogenated ethanes, HFC-134a, HCFC-123, and HCFC-141h, *Int. J. Thermophys.*, 1993, Vol. 14, P. 79-90.

43. M. J. Assael, E. Karagiannidis, Measurements of the thermal conductivity of R22, R123, and R134a in the temperature range 250-340 K at pressures up to 30 MPa, Int. J. Thermophys., 1993, Vol. 14, P. 183-197.
44. O. B. Tsvetkov, Yu. A. Laptev, A. G. Asambaev, Thermal conductivity of refrigerants R123, R134a, and R125 at low temperatures, Int. J. Thermophys., 1994, Vol. 15, P. 203-214.
45. U. Hammerschmidt, Thermal conductivity of a wide range of alternative refrigerants measured with an improved guarded Hot-Plate Apparatus, Int. J. Thermophys., 1995, Vol. 16, P. 1203-121.
46. S. T. Ro, J.Y. Kim, D. S. Kim, Thermal conductivity of R32 and Its mixture with R134a , Int. J. Thermophys., 1995, Vol. 16, P. 1193-1201.
47. . A. N. Gurova, U. V. Mardolcar, C. A. Nieto Castro, The thermal conductivity of Liquid 1,1,1,2-Tetrafluoroethane (HFC 134a), Int. J. Thermophys., 1997, Vol. 18, P. 1077-1087.
48. S. U. Jeong, M. S. Kim, S. T. Ro, Liquid thermal conductivity of binary mixtures of pentafluoroethane(R125) and 1,1,1,2-tetrafluoroethane (R134a), Int. J. Thermophys., 1999, Vol. 20, P. 55-62.
49. B. Le Neindre, Y. Garrabos, Measurements of the thermal conductivity of HFC-134a in the temperature range from 300 to 530 K and at pressures up to 50 MPa, Int. J. Thermophys., 1999, Vol. 20, P. 1379-1401.
50. A.V. Baginsky, A.S. Shipitsyna, Thermal conductivity and thermal diffusivity of the R134arefrigerant in the liquid state, Thermophys. Aeromech. 16 (2009) 267-273.
51. Y. Tanaka, S. Matsuo, S. Taya, Gaseous thermal conductivity of difluoromethane (HFC-32), pentafluoroethane (HFC-125), and their mixtures, Int. J. Thermophys., 1995, Vol. 16, P. 121-131.
52. M. J. Assael, L. Karagiannidis, Measurements of the thermal conductivity of liquid R32, R124, R125, and R141b, Int. J. Thermophys., 1995, Vol. 16, P. 851-865.
53. O. B. Tsvetkov, A. V. Kletski, Yu. A. Laptev, A. J. Asambaev, I. A. Zausaev, Thermal conductivity and PVT measurements of Pentafluoroethane (refrigerant HFC-125), Int. J. Thermophys., 1995, Vol. 16, P. 1185-1192.
54. U. Gross, Y. W. Song ,Thermal conductivities of new refrigerants R125 and R32 Measured by the Transient Hot-Wire method, Int. J. Thermophys., 1996, Vol. 17, P. 607-619.
55. S. T. Ro, M. S. Kim, S. U. Jeong,). Liquid thermal conductivity of binary mixtures of difluoromethane (R32) and pentafluoroethane (R125), Int. J. Thermophys., 1997, Vol. 18, P. 991-999.
56. S. H. Kim, D. S. Kim, M. S. Kim, S.T. Ro, The thermal conductivity of R22, R142b, R152a, and their mixtures in the liquid State, Int. J. Thermophys., 1993, Vol. 14, P. 937-950.
57. O. B. Tsvetkov, Yu. A. Laptev, A.G. Asambaev, The thermal conductivity of binary mixtures of liquid R22 with R142b and R152a at low temperatures, Int. J. Thermophys., 1996, Vol. 17, P. 597-606.

58. A.N. Gurova, U.V. Mardolcar, C.A. Nieto Castro, Thermal conductivity of 1,1-difluoroethane (HFC-152a), Int. J. Thermophys., 1999, Vol. 20, P. 63-72.
59. S.H. Lee, M.S. Kim, S.T. Ro, Thermal conductivity of 1,1,1-trifluoroethane (R143a) and R404A in the liquid phase, J. Chem. Eng., 2001, Vol. 46, P. 1013-1015.
60. X. Gao, Y. Nagasaka, A. Nagashima, Thermal conductivity of binary refrigerant mixtures of HFC-32/125 and HFC-32/134a in the liquid phase, Int. J. Thermophys., 1999, Vol. 20, P. 1403-1415.
61. V. Z. Geller, B.V. Nemzer, U.V. Cheremnykh, Thermal conductivity of the refrigerant mixtures R404A, R407C, R410A, and R507A, Int. J. Thermophys., 2001, Vol. 22, P. 1035-1043.
62. A.V. Baginsky, A.S. Shipitsyna, Thermal conductivity of liquid R507 refrigerant, Thermophys. Aeromech., 2008, Vol. 15, P. 291-295.
63. O.I. Verba, Thermal conductivity of refrigerant 507A in gaseous state*, Thermophys. Aeromech., 2011, Vol. 18, P. 151-154.
64. [66] X. Gao, Y. Nagasaka, A. Nagashima, Thermal conductivity of ternary refrigerant mixtures of HFC-32/125/134a in the liquid phase, Int. J. Thermophys., 1999, Vol. 20, P. 1417-1424.
65. S. U. Jeong, M.S. Kim, S.T. Ro,). Liquid thermal conductivity of ternary mixtures of difluoromethane(R32), pentafluoroethane (R125), and 1,1,1,2-tetrafluoroethane (R134a), Int. J. Thermophys., 2000, Vol. 21, P. 319-328.
66. O. I. Verba, E. P. Raschektaeva, S.V. Stankus, Experimental study of thermal conductivity of the R407C refrigerant in the vapor phase, High Temp., 2012, Vol. 50, P. 200–203.
67. O. I. Verba, Thermal conductivity of gaseous refrigerant R 404A*, Thermophys. Aeromech., 2007, Vol. 14, P. 165-168.
68. A.V. Baginsky, A. S. Shipitsyna, Thermal conductivity of liquid refrigerant R404A*, Thermophys. Aeromech., 2007, Vol. 14, P. 165-168.
69. T. Makita, Y.Tanaka, Y. Morimoto, M. Noguchi, H. Kubota, Thermal conductivity of gaseous Fluorocarbon refrigerants R 12, R 13, R 22, and R 23, under pressure, Int. J. Thermophys., 1981, Vol. 2, P. 249-268.
70. O. I. Verba, , E. P. Raschektaeva, S.V. Stankus, Thermal conductivity of refrigerant R-415A in the vapor phase , Thermophys. Aeromech., 2013, Vol. 20, P. 477-479.
71. O. I. Verba, E. P. Raschektaeva, S. V. Stankus, Experimental study of thermal conductivity of refrigerant R-409A in vapor phase*, Thermophys. Aeromech., 2011, Vol. 18, P. 661-664.

Table 1
The critical properties of compounds used in this work

Component	Molecular weight (g/mol)	T _c (K)	P _c (Mpa)	D _c (Kg/m ³)	Reference
R32	50.020	351.55	5.83000	430.0	[56]
R125	120.02	339.45	3.59000	571.0	[56]
R134a	102.00	374.18	4.05629	508.0	[49]
R152a	66.050	386.44	4.52000	365.0	[44]
R143a	84.040	346.25	3.81100	434.0	[44]
R22*	86.470	369.35	4.99000	513.0	[56]
R124*	136.48	395.65	3.63400	560.0	[44]
R142b*	100.50	410.25	4.24600	459.0	[44]
R152a*	66.050	386.44	4.52000	365.0	[44]

Table 2

Sources and ranges of data base used in this work for pure systems

Component	T (K)	P(Mpa)	X _i	(W. m. ⁻¹ K ⁻¹)		Reference
R134a	293.15-353.15	0.10-2.540	1	0.0123-0.0256	32	[37]
	272.46-400.47	0.1005-8.943	1	0.1165-0.0948	34	[38]
	202.83-303.05	1.2919-5.177	1	0.08445-0.1272	28	[39]
	253.25-363.15	0.096-6.097	1	0.01205-0.10605	76	[40]
	203.00-393.00	0.09-68.201	1	0.01036-0.14495	207	[41]
	273.15-363.15	0.10-2.8	1	0.01096-0.02036	38	[42]
	252.97-333.20	1.71-22.43	1	0.0707-0.1113	32	[43]
	169.87-290.06	10.00	1	0.0862-0.1430	19	[44]
	303.00-463.00	0.10	1	0.01376-0.02758	05	[45]
	223.15-323.15	2-25	1	0.07448-0.12087	24	[46]
	213.01-292.88	1.00-21.34	1	0.087297-0.13048	51	[47]
	232.75-323.25	2.00-20.00	1	0.0751-0.1184	23	[48]
R125	295.85-532.94	0.1-50.00	1	0.01276-0.10494	521	[49]
	295.85-354.95	1.379-4.147	1	0.05715-0.08401	102	[50]
R152a	172.74-290.02	10.00	1	0.0679-0.1116	16	[44]
	283.15-333.15	0.100-2.010	1	0.01229-0.01777	51	[51]
	253.04-313.46	1.24-16.03	1	0.0578-0.0793	19	[52]
	187.43-413.61	0.18-6.040	1	0.011-0.1075	28	[53]
	254.45-354.35	0.104-7.033	1	0.01212-0.08426	93	[54]
	231.25-324.05	2.00 -20.00	1	0.0524-0.0984	24	[55]
	231.25-324.05	2.00 -20.00	1	0.0524-0.0984	24	[48]
R32	283.15-333.15	0.10 -3.00	1	0.01084-0.02025	51	[51]
	252.67-312.83	3.68-17.63	1	0.1148-0.1704	21	[52]
	223.15-323.15	2.00-20.00	1	0.11035-0.1984	22	[46]
	233.45-334.95	0.098-6.194	1	0.01081-0.17762	55	[54]
	232.55-322.95	2.00-20.00	1	0.1141-0.1927	22	[55]
R143a	263.15-363.15	0.082-6.22	1	0.01215-0.1263	67	[40]
	223.15-323.15	2.1-20.1	1	0.0928-0.145	25	[56]
	303-423	0.1	1	0.01491-0.02592	4	[45]
	189.61-299.33	7.71-8.55	1	0.1076-0.159	11	[57]
	211.69-294.29	0.79-18.5	1	0.10259-0.14752	38	[58]

Table 3

Sources and ranges of data base used in this work for binary systems

Binary Systems	T (K)	P(Mpa)	X _i +X _j = 1	K(W. m. ⁻¹ K ⁻¹)	N	Reference
R32+R125	283.15-298.15	0.10-1.20	1876-0.8222	0.0117-0.01502	69	[51]
	232.65-323.95	2-20	0.2522-0.7595	0.0639-0.1667	120	[55]
	213-293	2-30	0.249-0.75	0.0814-0.1785	60	[60]
	255.04-409.8	0.101-3.69	0.5+0.5=1	0.02276-0.00998	50	[61]
R32+R134a	223.15-323.15	2-25	0.3057-0.7496	0.08165-0.17378	72	[46]
	193.2-316.1	2-30	0.249-0.75	0.0846-0.1953	84	[60]
R125+R134a	232.75-323.55	2-20	0.191-0.785	0.0597-0.1143	98	[48]
R507A	254.71-372.17	0.101-2.647		0.01007-0.02138	34	[61]
	297.95-332.55	1.465-3.775	0.5+0.5=1	0.05-0.0637	128	[62]
	312.59-424.24	0.105-1.902		0.01468-0.02528	79	[63]

Table 4

Sources and ranges of data base used in this work for ternary systems

Ternary systems	T (K)	P (Mpa)	+X _j +X _k = 1	K(W. m. ⁻¹ K ⁻¹)	N	Reference
R32+R125 +R134a	193.1-293	2-30	0.19-0.23	0.0797-0.144	44	[64]
	232.55-324.15	2-20	0.18-0.61	0.0641-0.1505	168	[65]
	253.27-389.83	0.101-2.447	0.23+0.25+0.52=1	0.00968-0.02012	38	[61]
	303.9-424.25	0.1055-2.038	0.23+0.25+0.52=1	0.0133-0.02454	97	[66]
407C	252.8-393.09	0.101-2.763	0.44+0.04+0.52=1	0.0099-0.02234	46	[61]
	233.55-322.95	2-20	0.44+0.04+0.52=1	0.0563-0.1056	24	[59]
	311.32-428.94	0.13-1.841	0.44+0.04+0.52=1	0.02584-0.01451	91	[67]
	297.85-332.65	1.277-3.818	0.44+0.04+0.52=1	0.05073-0.06532	108	[70]
404A	252.8-393.09	0.101-2.763	0.44+0.04+0.52=1	0.0099-0.02234	46	[61]
	233.55-322.95	2-20	0.44+0.04+0.52=1	0.0563-0.1056	24	[59]
	311.32-428.94	0.13-1.841	0.44+0.04+0.52=1	0.02584-0.01451	91	[67]
	297.85-332.65	1.277-3.818	0.44+0.04+0.52=1	0.05073-0.06532	108	[70]

N: Number of experimental data; **R410A** (R32, R125: 50%, 50%); **R507A** (R125, R143a: 50%, 50%),407C (R32, R125, R134a: 23%, 25%, 52%); **404A** (R125, R134, R143: 44%, 4%, 52%).

Table 5The values of coefficient of determination, R² and RMSE of different transfer function with the optimal number of neurons in each case

Type of Network	Input layer	Hidden layer	Output layer		
				Neurons Number	Activation function
Pure systems	FFBP	13	Logsig	Tansig	0.99312
	FFBP	16	Logsig	Purelin	0.99411
	FFBP	13	Tansig	Tansig	0.99615
	FFBP	19	Tansig	Purelin	0.98434
	FFBP	25	Purelin	Tansig	0.75703

Binary systems	FFBP	16	Logsig	Tansig	0.9971	0.0037
	FFBP	15	Logsig	Purelin	0.9956	0.0045
	FFBP	13	Tansig	Tansig	0.9980	0.0030
	FFBP	19	Tansig	Purelin	0.9911	0.0064
	FFBP	25	Purelin	Tansig	0.9909	0.0065
Ternary systems	FFBP	15	Logsig	Tansig	0.9934	0.0046
	FFBP	16	Logsig	Purelin	0.9928	0.0048
	FFBP	12	Tansig	Tansig	0.9983	0.0023
	FFBP	19	Tansig	Purelin	0.9933	0.0046
	FFBP	25	Purelin	Tansig	0.9080	0.0157
Global system(RN1)	FFBP	09	Tansig	Tansig	0.9925	0.0063
	FFBP	16	Logsig	Tansig	0.9941	0.0057
	FFBP	15	Logsig	Purelin	0.9825	0.0081
	FFBP	13	Tansig	Tansig	0.99667	0.0036
	FFBP	19	Tansig	Purelin	0.99279	0.0052
	FFBP	25	Purelin	Tansig	0.81528	0.0251

Table 6

Weights and biases of the optimal ANN architecture (Pure systems)

Input-Hiddenlayer							Output layer	
Weights(w_j^l)						Bias	Weights (w_j^h)	Bias
T	P	P_{PC}	T_{PC}	P_{PC}	D_{PC}	b_{hj}	λ	b_{OK}
4.1835	-26.0332	3.548	-0.73562	1.9594	-2.3406	-24.0384	8.1261	-1.078
3.1419	3.6054	-0.36381	-1.9651	-2.152	-4.9293	5.0308	-2.9587	
1.0815	-1.6325	0.4712	-0.27291	-0.90651	-1.3208	-2.0767	-0.78916	
-1.0815	0.8861	1.4178	1.1202	-1.3863	0.31068	0.21321	-1.852	
4.186	-27.8174	3.0948	-0.53317	1.8773	0.31068	-25.6167	-12.7112	
0.018849	-10.7969	-2.5628	-4.3041	4.3532	-5.1926	-3.7738	3.0238	
-2.758	-3.7144	-0.13042	-0.16113	-3.4486	-3.4213	-3.7011	-1.4468	
3.643	3.5253	1.06	1.6562	-1.7157	3.1487	-0.10328	1.4675	
0.20958	21.8944	7.2547	7.4236	-5.9335	7.6625	9.693	9.5999	
0.67147	-0.19387	1.7556	0.184331	0.37153	-0.39813	0.68139	-2.7786	
-3.7149	1.3188	-2.8947	-1.3753	-4.3276	-6.2882	-4.335	3.7792	
-4.7261	33.3708	9.3397	11.3213	10.045	11.4176	10.549	-4.4501	
1.7355	-0.72955	-0.66524	-0.53499	-1.8261	-1.2245	2.8832	1.4051	

Table 7

Weights and biases of the optimal ANN architecture (Binary systems)

Input-Hidden layer connections									
Weights(w_j^l)								Bias	
T	P	M_{PC}	T_{PC}	P_{PC}	D_{PC}	X_I	X_J	b_{hj}	

-1.1368	0.35087	0.061351	-0.092349	0.19155	0.015487	0.9552	0.93462	1.9505
-0.52848	-0.27209	-0.34413	1.5926	-1.8845	-2.2342	-0.89647	0.091077	0.72922
-9.2944	15.2025	-1.3931	-5.7894	-0.69764	-3.0922	-1.2185	0.63763	10.2253
0.74509	-0.046277	-2.1833	1.0658	1.6071	-1.7698	2.1854	-0.63659	-2.6666
-5.463	1.3739	0.35375	-3.044	-0.13265	3.0506	-0.70419	1.0513	0.063846
9.2908	-15.1812	0.67375	5.4099	0.5982	3.5809	0.51316	-0.9871	-9.9995
0.5417	-0.049875	-1.4994	1.3517	2.4231	-1.1869	2.38	-1.1708	-2.6427
-0.52533	-0.28921	1.232	2.1296	-1.0579	-2.9281	-0.47692	0.60561	0.72659
-5.2406	1.3486	1.0374	-3.6427	-1.5027	0.75957	-1.1621	0.60392	-0.0015349
-0.22325	-0.55471	-0.67886	-3.2055	0.02742	0.096161	1.0705	1.0084	-2.6841
-0.69205	0.062437	-0.88158	0.7745	0.60294	1.371	-0.51057	-0.9332	-1.8227
3.4761	21.2807	0.9883	1.1499	-0.0055736	-0.49002	0.76189	0.62307	21.9264
3.4725	12.7136	0.97232	1.2258	0.24431	-0.20199	0.64987	0.51264	14.4721
Hidden layer -Output connections								
Neuron	1	2	3	4	5	6	7	8
Weights (w_j^h)	2.1988	2.5544	-3.6827	1.0359	0.43907	-3.6939	-1.1012	-2.4532
Neuron	9	10	11	12	13	Bias (b_{OK})		
ghts(w_j^h)	-0.44522	-0.52743	3.8007	8.5022	-8.5843	0.80292		

Table 8
Weights and biases of the optimal ANN architecture (Ternary systems)

Input-Hidden layer connections											
Weights(w_j^I)								Bias			
T	P	M _{PC}	T _{PC}	P _{PC}	D _{PC}	X _I	X _J	X _K	b _{hj}		
-6.7739	31.4165	3.2577	0.39732	1.036	-2.527	-3.2365	-4.0231	-2.7244	25.5898		
-0.29425	-0.9485	-0.21473	0.21213	1.2451	-0.7214	0.11886	-0.74649	-2.0618	3.0249		
-2.47	0.18387	0.75536	1.8232	0.99324	-0.27279	0.11747	1.3872	-0.52704	-1.2649		
6.7677	-0.902	0.55508	-0.22995	-0.18338	1.1255	-0.24203	-0.49338	0.82683	-1.0511		
12.3596	-35.956	-3.9554	-1.2256	-0.82614	2.2185	3.2681	5.1516	3.3689	-28.9329		
-8.6059	30.2842	3.1171	0.62656	0.4441	-3.11	-3.9329	-4.3703	-3.1823	24.2517		
5.3871	-0.45338	0.17102	0.88106	1.5367	0.51125	-0.22673	0.45733	-0.37837	0.89032		
-4.024	0.6629	-0.072903	0.8168	1.6132	0.075941	-0.90256	0.61739	-0.52554	0.30976		
-0.55489	0.97025	0.81368	-1.2384	-1.1274	0.27533	-0.68395	2.6689	-0.7989	-0.52271		
-1.9379	0.18981	-0.039593	-0.46625	-1.1118	-0.55954	1.1551	0.28289	0.45203	-1.8192		
-0.93241	0.1198	-1.3877	-0.25618	-0.12932	0.32091	0.38547	0.91658	-0.77965	-2.7939		
-1.7399	0.087514	0.91754	0.57086	-0.14689	0.19638	0.45431	-0.51917	-0.50043	-0.42572		
Hidden layer -Output connections											
Neuron	1	2	3	4	5	6	7				
Weights(w_j^h)	5.5039	0.16279	2.6773	0.11532	-5.1089	-9.9932	0.33928				
Neuron	8	9	10	11	12	Bias (b_{OK})					
Weights (w_j^h)	0.45079	0.36474	3.0944	-1.4005	-2.6727	1.1341					

Table 9

Parameters (weight and bias) of the ANN of global systems (pure systems +Binary systems +Ternary systems)

Input-Hidden layer connections									
T	P	b _c	c	b _c	c			X _K	Bias
6.957	-12.2166	2.9853	-1.3155	2.0151	-2.1339	3.3188	2.9528	2.015	-9.5758
1.4863	0.65639	-3.5468	-3.212	-0.67515	-5.9821	5.0425	-6.9349	3.4699	-3.1199
10.335	-81.7504	6.0135	-1.6097	4.2269	-3.718	17.1393	16.9112	12.3423	-63.1976
11.5506	-19.1889	1.0367	-2.2234	-4.1378	-10.7707	0.96966	6.8634	4.6281	-15.8314
-5.1279	1.2623	7.8443	5.3259	-5.9467	5.445	-8.7607	11.7747	-4.9305	-1.0918
1.4196	0.70906	-5.2684	-3.4587	-1.2712	-5.6834	6.5972	-7.3254	4.5641	-3.5073
-10.6208	23.0268	-10.2401	2.4067	-6.6956	6.7064	-4.5555	-4.6063	-3.5096	14.769
1.1016	-1.1453	-9.782	0.29611	-5.9066	6.0638	0.4596	0.41237	0.30055	-1.9767
10.1973	-21.9597	9.7397	-2.2774	6.3447	-6.3376	4.2893	4.3408	3.3243	-14.2148
-0.81496	0.045279	-1.263	0.050917	-0.43153	0.67735	-0.233	-0.21751	-0.17218	-2.5694
-5.9358	41.3513	-5.2625	1.0139	-2.699	3.4824	-8.3715	-8.3472	-6.1807	31.8419
-5.8418	41.3729	-4.9489	0.9846	-2.5971	3.2643	-7.8934	-7.8601	-5.8206	32.3549
-7.2882	13.0275	-2.485	3.8655	-2.1155	8.6409	0.18179	-2.7696	-1.5401	10.0868
Hidden layer -Output connections									
Neuron	1	2	3	4	5	6	7		
Weights(w _j ^h)	0.5244	-1.9121	-2.2127	0.4186	-0.034145	1.8947	-5.637		
Neuron	8	9	10	11	12	13		Bias (b _{OK})	
Weights (w _j ^h)	0.21922	-6.1822	11.9478	7.0574	-9.0366	0.49239	11.0953		

Table 10

Linear regression vectors (linear equation: $\gamma^{cal} = \alpha\gamma^{exp} + \beta$, with, α = slope β = y intercept, R^2 correlation coefficient)

Systems	N		α	β	R^2
Pure systems	1817	Training phase	1.000	0.00120	0.99667
		Validation phase	1.000	0.00120	0.99539
		Test phase	0.990	0.00030	0.9944
		Total	1.000	0.00096	0.99615
Binary systems	794	Training phase	1.000	0.00120	0.99810
		Validation phase	1.000	0.00094	0.99790
		Test phase	1.000	0.00130	0.99780
		Total	1.000	-0.00120	0.99800
Ternary systems	616	Training phase	1.000	0.0001100	0.99810
		Validation phase	1.000	0.0001700	0.99910
		Test phase	1.000	0.0002900	0.99880
		Total	1.000	0.0000064	0.99830
Global systems (RN1)	3227	Training phase	1.000	0.00054	0.99668
		Validation phase	1.000	0.00067	0.99641
		Test phase	1.000	0.00071	0.99690
		Total	1.000	0.00058	0.99667

Table 11**The values of the different errors of this study**

Systems	RMSE	MSE	AAD	AARD%	SSE	R^2_{Cal}
Pure systems	0.0027	0.0000	0.0024	07.6812	0.0244	0.9977
Binary systems	0.0030	0.0000	0.0020	07.4144	0.0074	0.9988
Ternary systems	0.0023	0.0000	0.0013	04.8599	0.0033	0.9989
Global system(RN1)	0.0036	0.0000	0.0023	08.1295	0.0411	0.9980

Table 12**Linear regression vectors and error performance between models obtained by RN1, RN2, RN3**

	α	β	R^2_{exp}	RMSE	MSE	AAD	AARD%	SSE	R^2_{cal}
RN1	01.000	0.00058	0.99667	0.0036	0.0000	0.0023	08.1295	0.0411	0.9980
RN2	01.000	-0.00082	0.99805	0.0027	0.0000	0.0018	05.2531	0.0237	0.9988
RN3	01.000	-0.00330	0.99683	0.0035	0.0000	0.0023	07.7516	0.0393	0.9981

Table 13**Sources and ranges of new data base for pure systems.**

Pure Systems	T (K)	P(Mpa)	X _i = 1	K(W. m. ⁻¹ K ⁻¹)	N	Reference
R22	298.15-393.15	0.1-5.76	1	0.0106-0.0682	130	[69]
	252.48-333.32	0.1-26.58	1	0.0667-0.1141	37	[43]
	223.15-323.15	2.1-20.1	1	0.0713-0.1262	50	[57]
	303-463	0.1	1	0.01089-0.02064	05	[45]
	208.56-289.6	0.9	1	0.0875-0.1222	16	[58]
R142b	293.15-353.15	0.1-1.35	1	0.0109-0.0165	21	[37]
	302.201-304.346	1.6425-69.5827	1	0.08064-0.11163	32	[39]
	223.15-323.15	2.1-20.1	1	0.0734-0.1183	25	[57]
	298-418	0.1	1	0.01249-0.0214	05	[45]
	210.4-289.55	4.31-7.59	1	0.0872-0.1164	07	[58]
R124	252.4-333.1	0.62-18.67	1	0.0584-0.0909	35	[52]

Table 14**Sources and ranges of new data base for binary systems**

Binary Systems	T (K)	P(Mpa)	X _i +X _j = 1	K(W.m. ⁻¹ K ⁻¹)	N	Reference
R22+R142b	223.15-323.15	2.1-20.1	0.2796-0.729	0.01664-0.1207	75	[57]
	164.77-295.76	2.7-8.14	0.377-0.765	0.0854-0.1422	16	[58]
R22+R152a	223.15-323.15	2.1-20.1	0.2488-0.750	0.0759-0.1391	75	[57]
	176.6-297.45	2.44-8.02	0.269-0.765	0.0916-0.1512	13	[58]
R415	308.22-415.55	0.12-1.684	0.5+0.5=1	0.0139-0.0225	61	[70]

Table 15

Sources and ranges of new data base for ternary systems

Ternary Systems	T (K)	P(Mpa)	$X_i+X_j+X_k=1$	$K(W \cdot m^{-1} K^{-1})$	N	Reference
R409	305.67-427.13	0.0591-1.364	0.15+0.25+0.6=1	0.0118-0.0196	57	[71]

N: Number of experimental data; **R415** (R22, R152a: 50%, 50%); **R409** (R142b, R124, R22: 15%, 25%, 60%).

Table 16

Comparison between the prediction model of different results of new data base (DB2) obtained by each model RN1, RN2, RN3

Model	Systems	N	RMSE	MSE	AAD	ARD%	SSE	R^2_{Cal}
RN1	Pure	363	0.0284	0.0008	0.0212	48.7426	0.2925	0.8446
	Binary	240	0.0116	0.0002	0.0094	21.046	0.0486	0.9754
	Ternary	57	0.0304	0.0009	0.0202	115.911	0.0525	-2.7634
	Total	660	0.0244	0.0006	0.0169	44.7115	0.3936	0.8982
RN2	Pure	363	0.0218	0.0005	0.0147	23.0868	0.1723	0.9084
	Binary	240	0.0167	0.0004	0.0121	23.2145	0.1017	0.9484
	Ternary	57	0.0021	0.0000	0.0017	10.8684	0.0002	0.9827
	Total	660	0.0204	0.0004	0.0126	22.0780	0.2743	0.9291
RN3	Pure	363	0.0140	0.0002	0.0108	21.1563	0.0710	0.9623
	Binary	240	0.0090	0.0001	0.0092	14.6979	0.0292	0.9853
	Ternary	57	0.0020	0.0000	0.0017	10.8850	0.0002	0.9832
	Total	660	0.0123	0.0002	0.0094	17.9208	0.1004	0.9742

Table 17

Statistical analyses of the error of the predicted results (RN4).

System	N	MSE	MSE	AAD	AARD%	SSE	R^2_{Cal}
DB1+DB2	3887	0.0028	0.0000	0.0018	5.78	0.0303	0.9988

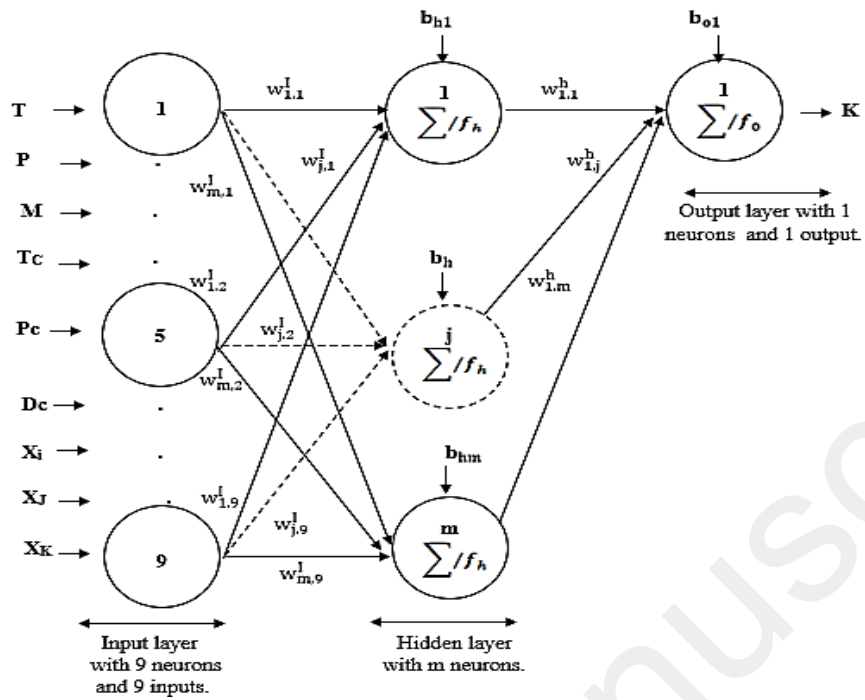


Fig.1.Feed forward neural network for the prediction of thermal conductivity of refrigerants.

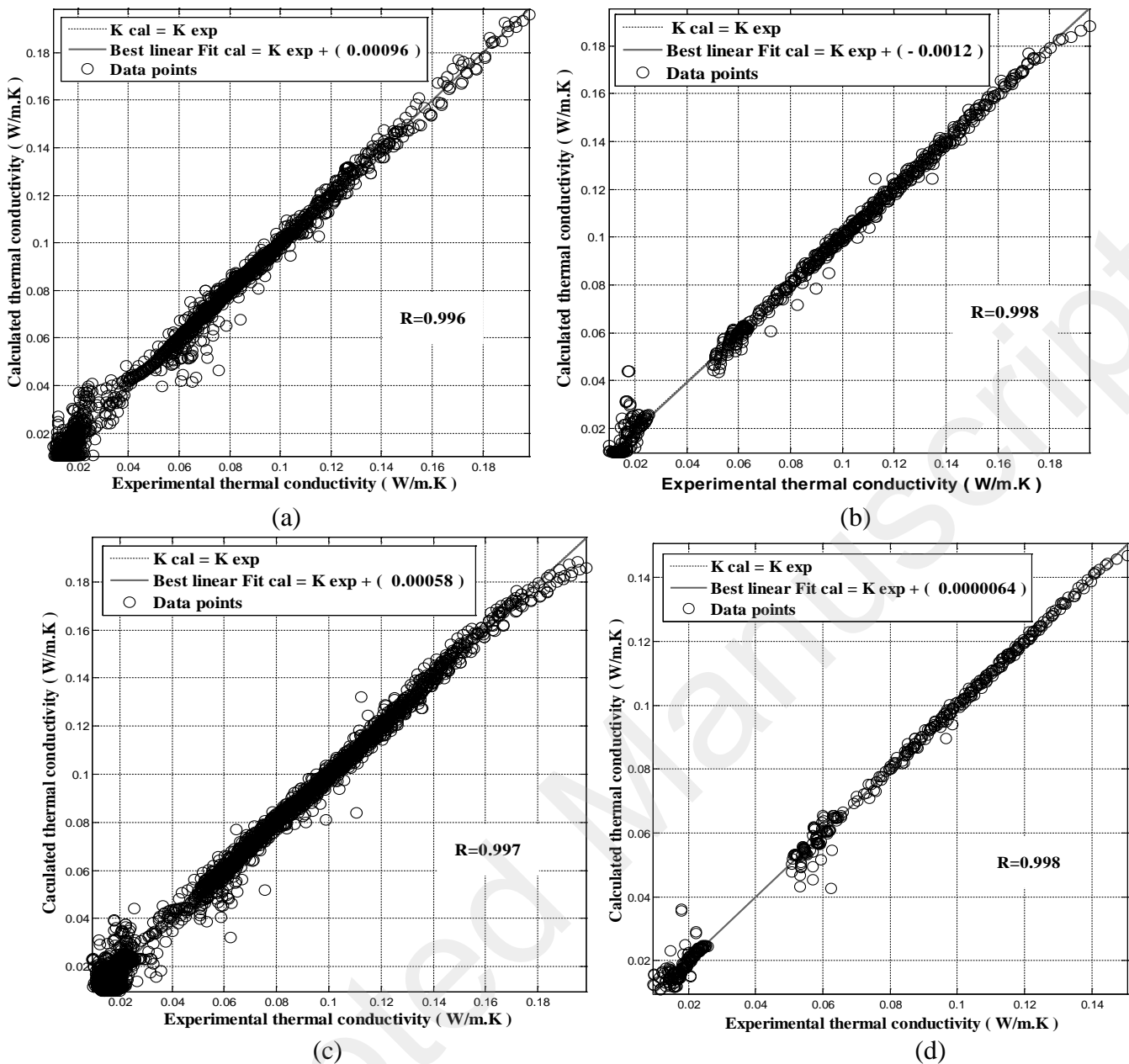
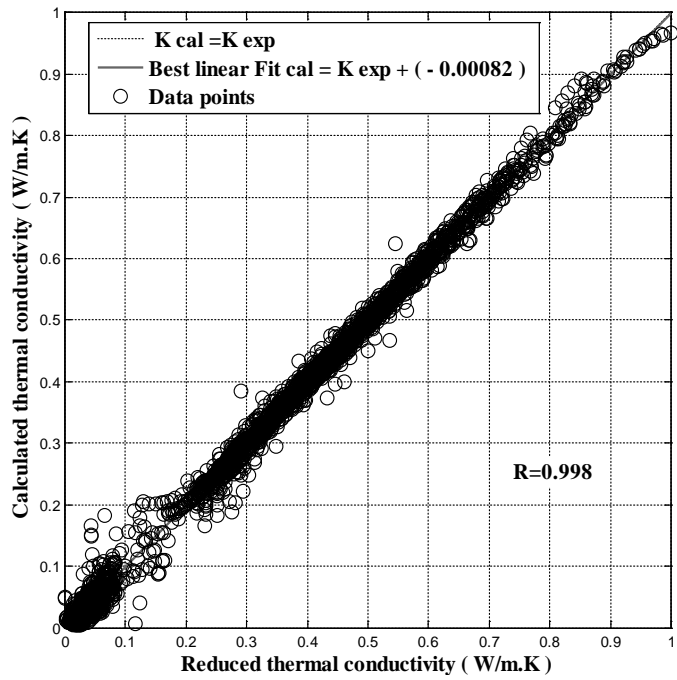
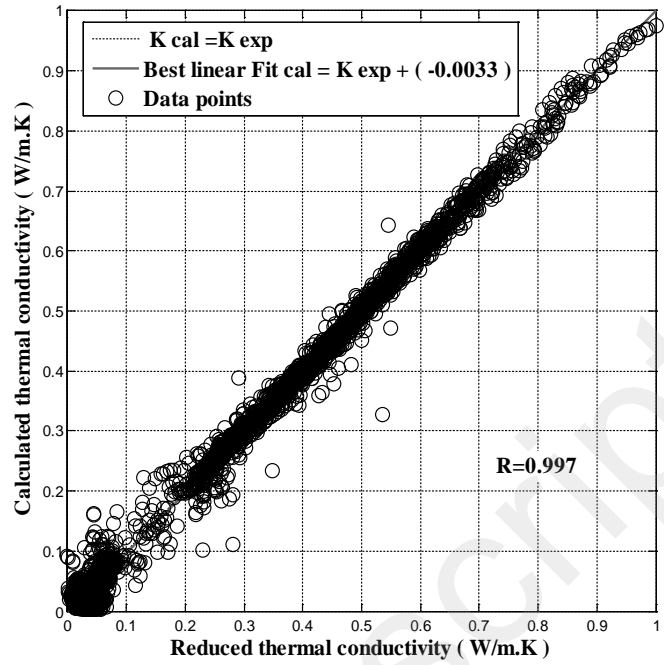


Fig. 2. Comparison of experimental and calculated values for the whole data set (a) Pure systems, (b) Binary systems, (c) Ternary systems, (d) Global system.



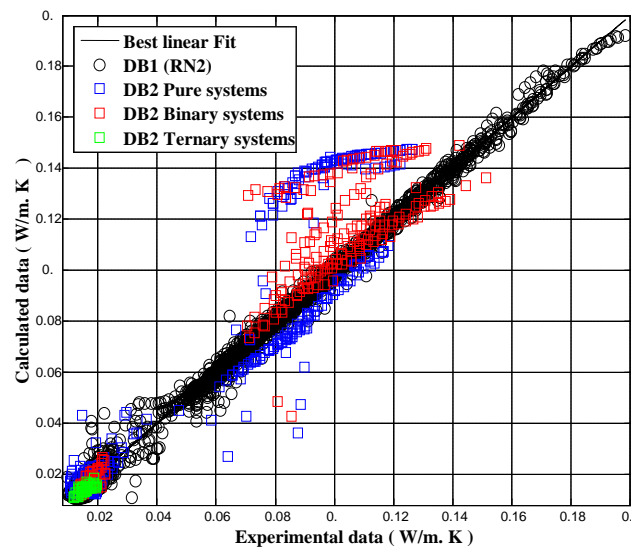
(e)



(f)

Fig. 3. Comparison of reduced and calculated values for the whole data set: (e) RN2 (number of neurons=17), (f) RN3 (number of neurons=13) for global system.

(a)



(c)

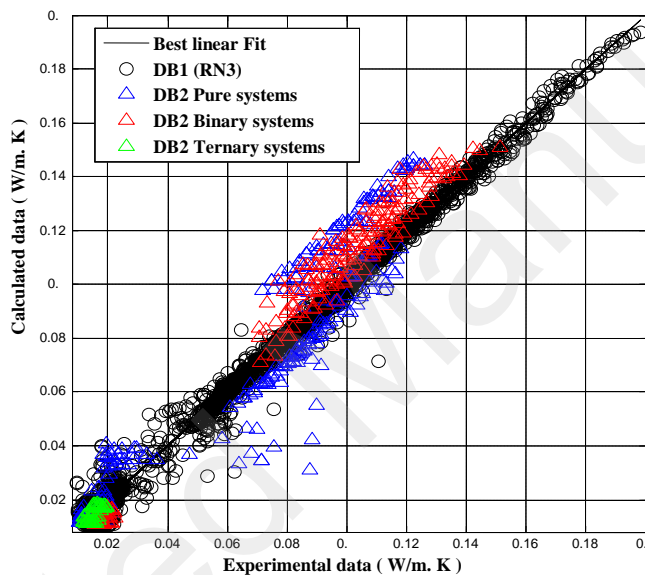


Fig.4.Comparison between data base DB1and DB2 for pure, binary and ternary systems:(a) RN1, (b) RN2, (c), RN3, for the prediction model.

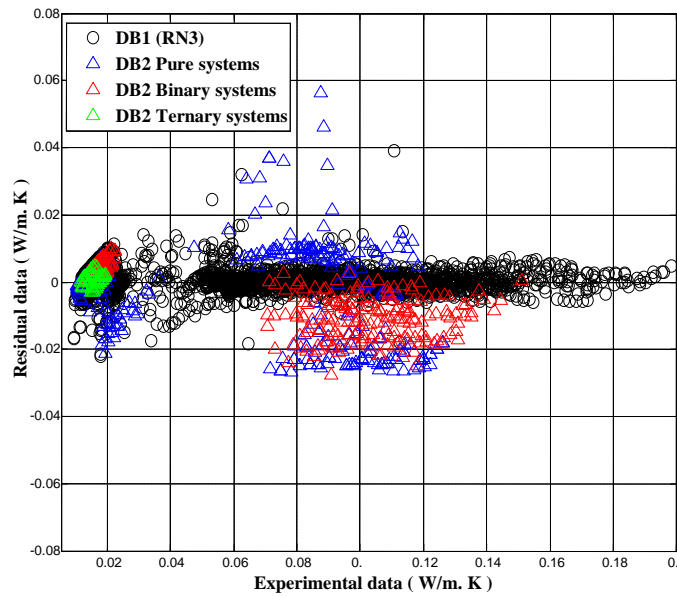


Fig.5. Plot of the residuals for calculated values of thermal conductivity from the ANN model versus their experimental values for DB2, [Residual = $K_{exp,i} - K_{cal,i}$].

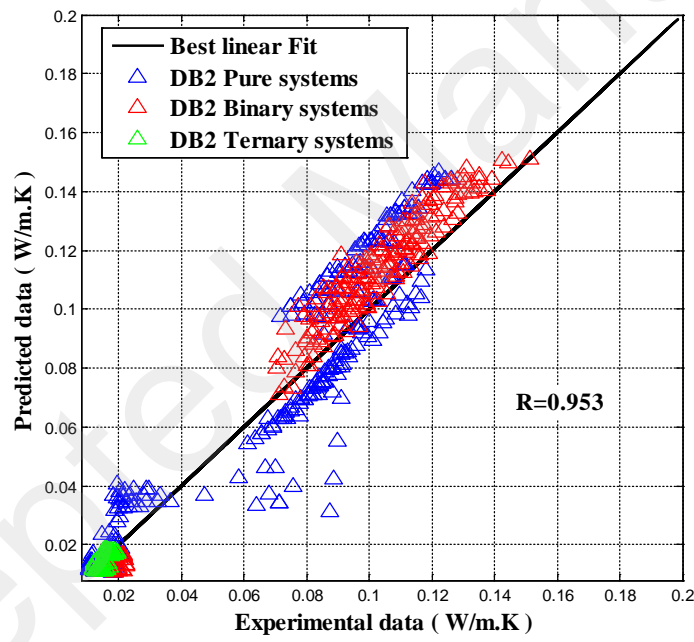


Fig.6. Prediction of the new data base DB2.

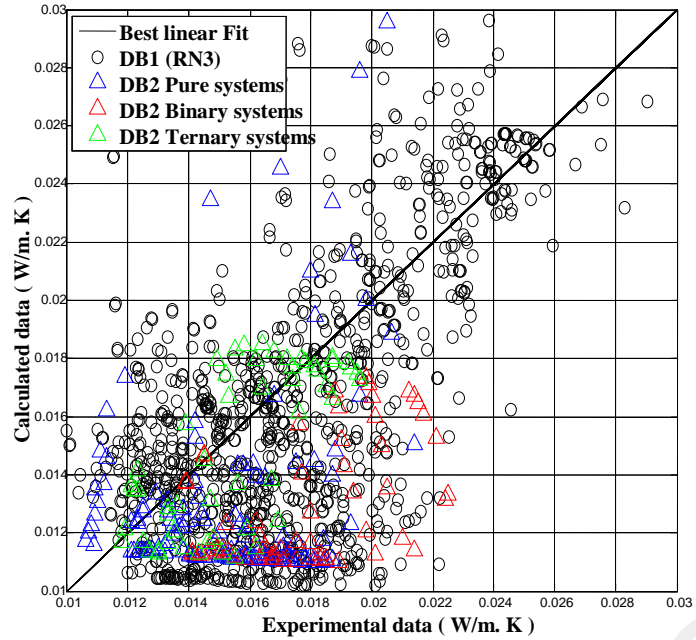


Fig. 7.The prediction between the DB2 and the actual data base DB1 in the range [0.01, 0.03].

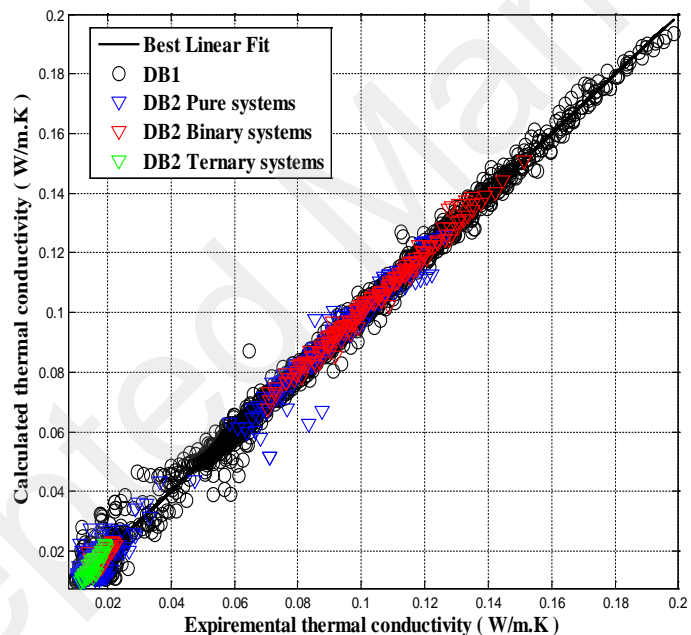


Fig. 8.Regression analysis plot for the optimal model between output and target of thermal conductivity(RN4).

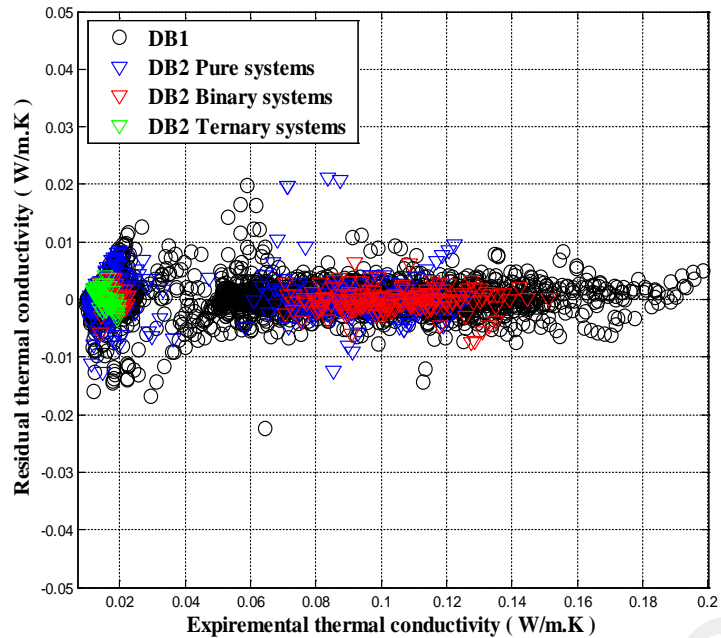


Fig. 9. Plot of the residuals for calculated values of thermal conductivity from the ANN model and their experimental data points (RN4).